Contemporary Mathematics
http://ojs.wiserpub.com/index.php/CM/

Research Article

Assessing the Efffects of Vaccination on Tuberculosis and COVID-19 Co-Infection Modelling

Harshita Kaushik[1*], V. S. Verma[1], Ram Singh[2], A. Manickam[3]

[1]Department of Mathematics and Statistics, Deen Dayal Upadhyaya Gorakhpur University, Gorakhpur, Uttar Pradesh, 273009, India
[2]Department of Mathematical Sciences, Baba Ghulam Shah Badshah University, Jammu & Kashmir, 185234, India
[3]School of Sciences, Division of Mathematics, SRM Institute of Science and Technology (SRMIST), Tiruchirappalli Campus, Tiruchirappalli, 621105, Tamilnadu, India
E-mail: harshitakaushik1395@gmail.com

Received: 15 September 2023; **Revised:** 3 November 2023; **Accepted:** 15 November 2023

Abstract: In this paper, an epidemiological model is proposed to study the dynamics of coinfection diseases (TB) and COVID-19 with the effect of vaccination. Tuberculosis (TB) and COVID-19 both are infectious diseases that pose significant global health challenges. Evidence suggests that individuals with TB have a higher risk of acquiring the COVID-19 infection. With the emergence of the COVID-19 pandemic, concerns have arisen regarding the potential impact of the concomitant presence of TB and COVID-19. The epidemiological model is qualitatively analysed using stability analysis theory. The dynamic system exhibits a stable endemic equilibrium point while $R_0 < 1$ and unstable when $R_0 > 1$. The Lyapunov function is used to investigate the global stability of an endemic equilibrium point. The sensitivity analysis is carried out to identify the effective parameters that have the greatest influence on the reproduction number. Numerical results are carried out to assess the effect of various biological parameters in the dyanamic of both coinfection classes of TB & COVID-19. This study aims to analyze the implications of these concurrent diseases and predict the effect of vaccination in managing their coexistence. Our simulation results show that both the coinfection disease TB and COVID-19 can be reduced by increasing rate of vaccination.

***Keywords*:** TB, COVID-19, vaccination, sensitivity analysis

MSC: 92C12, 34A34, 26A33, 92D30

Nomenclature

A: Inflow rate.
α_1: TB infection population mortality rate due to disease.
α_2: COVID-19 infection population mortality rate due to disease.
α_3: Case fatality rate (CFR) of TB and COVID-19 co-infection.
β_0: TB propagation rate.
β_1: COVID-19 propagation rate.

DOI: https://doi.org/10.37256/cm.6120253677

ζ_1: Recovery rate of TB infectives from TB population.
ζ_2: Recovery rate of COVID-19 infectives from COVID-19 population.
ζ_3: Recovery rate of coinfection of TB and COVID-19 infectives from coinfection of TB and COVID-19 population.
μ: Rate of natural mortality.
ψ: Rate of COVID-19 Vaccination.
θ: Failure rate of COVID-19 Vaccination.
η: Rate of BCG Vaccination.

1. Introduction

The COVID-19 virus, which originated in Wuhan, China in late 2019, silently proliferated across numerous countries until March 2020, causing a global crisis. From April 5, 2020 onwards, every nation has been grappling with the impact of this deadly virus, as it spreads from asymptomatic individuals to susceptible populations [1, 2].

The initial outbreak was identified in China's Wuhan region [3]. In light of this, COVID-19 has spread worldwide. To combat the pandemic, numerous countries implemented lockdown measures followed by gradual easing of restrictions, considering political ramifications and their impact on socio-economic conditions [4–8]. Quarantine, isolation, and social distancing were among the primary non-pharmaceutical interventions (NPIs) implemented as the initial line of defense against the virus [9, 10]. People transmit COVID-19 by means of respiratory droplets, either through direct contact with contaminated surfaces or by coming into contact with individuals who are infected [11]. While the majority of SARS-CoV-2 infections tend to resolve on their own with mild symptoms, it is widely recognized that individuals who are older and have pre-existing conditions such as hypertension, diabetes, tuberculosis (TB), and coronary heart disease are at a significantly higher risk of experiencing severe complications and mortality from COVID-19 [12–14]. The tireless endeavors of numerous scientists have resulted in the successful development of vaccines to safeguard against COVID-19, bringing about a fortunate outcome [6].

Both COVID-19 and tuberculosis are transmitted through a common pathway in the human body, specifically via the upper respiratory tract [15–17].

Tuberculosis (TB) ranks among the top 10 causes of global mortality. The illness, primarily affecting the lungs, stems from the activity of Mycobacterium tuberculosis bacteria [18]. TB is both preventable and curable. It spreads through airborne transmission when individuals with lung TB cough, sneeze, or spit, releasing the TB bacteria into the air [18]. Inhaling just a few of these bacteria can lead to infection [19]. An environmental aspect that contributes to the spread of TB is the discharge of domestic wastes, open water storage tanks, and open sewage drains in residential areas. Globally, an estimated ten million new cases of tuberculosis were reported in 2017 [20].

It's worth noting that approximately one-third of the world's population has latent TB, signifying that they have been infected by TB bacteria but are not yet experiencing symptoms and are incapable of transmitting the disease [21].

Mathematical models play an essential role in epidemiology, the study of disease spread and control within populations. Mathematical models aid epidemiologists in understanding disease transmission dynamics. These models shed light on how illnesses spread and evolve by simulating the interactions of infected, susceptible, and recovered individuals. Epidemiological models can forecast the future course of an epidemic or pandemic, including the predicted number of cases, peak infection time, and the effectiveness of control efforts. This data is necessary for public health planning and resource allocation. Models enable researchers to evaluate the effectiveness of various interventions like as vaccination campaigns, social distancing measures, and quarantine techniques. This enables policymakers to make informed judgments about how to control disease transmission. Models enable researchers to evaluate the effectiveness of various interventions like as vaccination campaigns, social distancing measures, and quarantine techniques. This enables policymakers to make informed judgments about how to control disease transmission. Keeping this in mind formulation of a coinfection model is done to study the impact of vaccination to control the disease. The model is developed by the authors for the first time. However, different mathematical models were used to construct this model [22–24].

Tuberculosis and COVID-19 have distinct clinical presentations, modes of transmission, and treatment strategies. However, their co-existence can complicate diagnostic procedures, disease management, and overall health outcomes [25]. This section provides an overview of TB and COVID-19, highlighting their individual characteristics and discussing the potential challenges when they occur simultaneously the interactions between TB and COVID-19, including the impact of one disease on the other. The potential implications of TB infection on COVID-19 severity and vice versa are examined. Vaccination has played a crucial role in controlling infectious diseases throughout history [26, 27]. This section reviews the existing TB and COVID-19 vaccines and their efficacy in preventing. Moreover, it explores the potential benefits of vaccination in individuals with concomitant TB and COVID-19 infections. Using available data, this section employs modeling and predictive analysis techniques to estimate the potential impact of vaccination strategies in managing TB and COVID-19 coexistence. It considers variables such as vaccine coverage, vaccine effectiveness [28].

Based on the analysis and predictions, this section discusses the implications for public health policies and practices. It emphasizes the importance of targeted vaccination campaigns, prioritizing high-risk populations, and optimizing resources to effectively control the spread of both TB and COVID-19.

The goal of this research is to identify the number of TB patients infected by COVID-19 and the number of serious illnesses during the COVID-19 pandemic [29].

This study highlights the significance of understanding the interactions between TB and COVID-19 and the potential benefits of vaccination strategies [30]. By analyzing available data and employing predictive modeling, we can gain valuable insights into the expected outcomes of vaccination in managing these concomitant diseases. These findings can inform public health efforts, aid policymakers, and contribute to the development of effective strategies for combating TB & COVID-19 coexistence (Table 1).

The order of the paper is as follows: Section 2 is dedicated to the formulation of mathematical models. Section 3 contains the basic preliminary details of the suggested model. Section 4 performs the analysis of mathematical model. In section 5 parametric variation of R_0 is explained. In section 6, sensitivity analysis has been carried out. The numerical results are given in section 7. The conclusion is given in section 8.

Table 1. Comparative analysis of related works of TB & COVID-19 co-dynamics

Authors	Key findings	Mortality from coinfection	Recommendations
Visca et al. [31]	COVID-19 may occur before, during, or after a TB diagnosis.	This is more likely to occur in elderly patients with comorbidities.	More research is needed to determine the possible impact of COVID-19 on TB patients.
Chen et al. [32]	MTB infection increases the susceptibility to SARS-CoV-2 and the severity of COVID-19.	-	It will be important to validate the relationship uncovered here in 36 COVID-19 cases in a large study.
Khurana and Aggarwal [33], Tadolini et al. [34]	Due to the chronic nature of TB, patients will have more time to become infected with COVID-19.	12.3% mortality in the patients with dual infection.	In the fight against COVID-19 it is important to suspect and manage TB.
Goudiaby et al. [35]	Because of their geographical overlap, coinfection of these diseases is unavoidable, posing a potential double blow because clinical similarities may impede measures to control their spread.	-	Study on exogeneous TB re-infection and COVID-19 re-infection after recovery (as various variations have recently emerged).

2. Mathematical model

In this chapter, a deterministic compartment model is proposed to study and analyse the dynamics of two concomitant diseases TB and COVID-19. For the formulation of the model, we have divided the whole population into five compartments based on their status that are mutually distinct epidemiological states. Let, $S(t)$ indicates the population which is susceptible for COVID-19 and TB, $T(t)$ denotes the population infected by TB infectives only, $C(t)$ indicates the population infected by COVID-19 only, $B(t)$ is the co-infection population of both TB and COVID-19 and $V(t)$ indicates the vaccination compartment. Let $N(t)$ represents the entire population (the sum of five subpopulations) at any given time 't'. Therefore, we have $N(t) = S(t) + T(t) + C(t) + B(t) + V(t)$.

Schematic representation of the proposed model is shown in Figure 1.

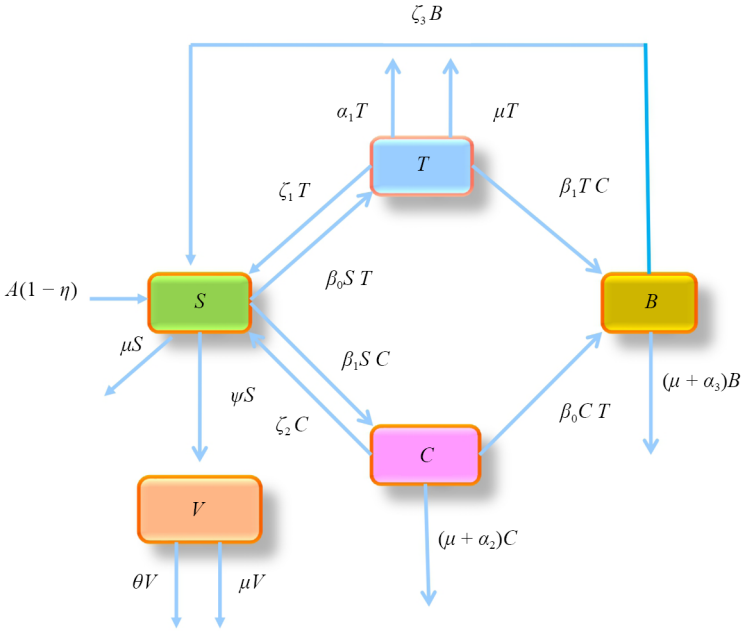

Figure 1. Schematic representation of compartment model

The proposed model is based on the traditional SIS model since it assumes that the individuals who have recovered from the virus will re-enter the susceptible class. Now, let the susceptible population enter in the system at a steady rate $A(1-\eta)$. Also, the susceptible class is vaccinated with COVID-19 vaccination at vaccination rate ψS. The susceptible population is transitioning at the propagation rate β_0 to the TB infected class $T(t)$ and infected class $C(t)$ of COVID-19 at the propagation rate β_1. When patients with TB comes into contact with COVID-19 patients and acquire the disease, they are categorised as the coinfected class $B(t)$ with both diseases COVID-19 & TB. Also, when COVID-19 acquires infected population TB, they moves to $B(t)$. Furthermore, TB patients recover at a rate of ζ_1, COVID-19 patients recover at a rate of ζ_2, and the population infected with TB and COVID-19 after recovery re-enters the susceptible population at a rate of ζ_3. Further, α_1, α_2, and α_3 are assumed to be the case fatality rate of TB, COVID-19 and both TB & COVID-19 infected population respectively. Let μ is the rate of natural mortality rate of population and θ is supposed to be the failure rate of COVID-19 vaccination.

The mathematical formulation of the propsed model is described below:

$$\left.\begin{aligned}
\frac{dS}{dt} &= A(1-\eta) + \zeta_1 T + \zeta_2 C + \zeta_3 B - \beta_0 ST - \beta_1 SC - \mu S - \psi S,\\
\frac{dT}{dt} &= \beta_0 ST - \beta_1 TC - (\zeta_1 + \mu + \alpha_1) T,\\
\frac{dC}{dt} &= \beta_1 SC - \beta_0 CT - (\mu + \alpha_2 + \zeta_2) C,\\
\frac{dB}{dt} &= \beta_0 CT + \beta_1 TC - (\mu + \alpha_3 + \zeta_3) B,\\
\frac{dV}{dt} &= \psi S - \theta V - \mu V,
\end{aligned}\right\}, \tag{1}$$

with the following initial conditions:

$$S(0) = S_0 \geq 0,\ T(0) = T_0 \geq 0,\ C(0) = C_0 \geq 0,\ B(0) = B_0 \geq 0,\ V(0) = V_0 \geq 0. \tag{2}$$

3. Positivity and boundedness of the model

Non-negativity conditions are necessary to show that all the state variables remain positive for $t \geq 0$ or the solutions of the system remain positive for all time. Thus, we have the following theorem:

Theorem 2.1 Under the initial conditions given by (2), all the solutions (S, T, C, B, V) of model (1) fullfills $S(0) > 0$, $T(0) \geq 0$, $C(0) \geq 0$, $B(0) \geq 0$ and $V(0) \geq 0$ for which the solutions of the model stay positive for all time $t \geq 0$.

Proof. From (1) and (2), it can be easily seen that

$$\left.\frac{dS}{dt}\right|_{S=0} = A(1-\eta) + \zeta_1 T + \zeta_2 C + \zeta_3 B > 0, \tag{3}$$

$$\left.\frac{dT}{dt}\right|_{T=0} = 0, \tag{4}$$

$$\left.\frac{dC}{dt}\right|_{C=0} = 0, \tag{5}$$

$$\left.\frac{dB}{dt}\right|_{B=0} = \psi S - V(\theta + \mu) > 0. \tag{6}$$

From the above, we conclude that, all solutions (S, T, C, B, V) of the proposed co-infection model TB and COVID-19 remain positive for all $t \geq 0$.

Now, we shown that the solutions to the system of equations (1) are bounded. The term "boundedness" refers to the natural limits on the growth of the infected population resulting from various constraints, such as environmental factors or preventative behaviors adopted to prevent from the disease.

Now, we demonstrate the following theorem:

Theorem 3.2 The set $\Lambda = \{(S, T, C, B, V)\colon 0 \leq S+T+C+B+V \leq N\}$ is closed area for the system (1), where all solutions start in the positive octant with non-negative initial conditions, where $N_P = \dfrac{A(1-\eta)}{\mu+\psi}$.

Proof. Summing equations of the system (1) and using the relation $N = S+T+C+B+V$, we get

$$\frac{dN}{dt} = A(1-\eta) - \mu N - \alpha_1 T - \alpha_2 C - \alpha_3 B - \theta V. \tag{7}$$

$$\frac{dN}{dt} \leq A(1-\eta) - \mu N.$$

By comparison principle, we can write

$$0 < N \leq \frac{A(1-\eta)}{\mu+\psi}. \tag{8}$$

Thus, the set $A = \{(S, T, C, B, V)\colon 0 \leq S+T+C+B+V \leq N\}$ is closed region for the system (1) as well as all solutions of the model is contained in the set A.

Thus, in the above defined set A, the coinfection model of TB & COVID-19 is well-defined biologically and mathematically.

4. Existence of equilibrium points

Here, we search for the existence of equilibrium points of the proposed model. The existence of unique positive equilibrium point and stability of system (1) depends on the basic reproductive number R_0 at disease free equilibrium point, which is determined with the help of the next generation matrix method [36]. Clearly, the system (1) contains the two equilibrium points: the first one is disease free equilibrium point $\left(\dfrac{A(1-\eta)}{\mu}, 0, 0, 0, \dfrac{\psi S}{\theta+\mu}\right)$ and the other endemic equilibrium point $(S^*, T^*, C^*, B^*, V^*)$.

The following equations must be satisfied by the endemic equilibrium point:

$$A(1-\eta) + \zeta_1 T^* + \zeta_2 C^* + \zeta_3 B^* - \beta_0 S^* T^* - \beta_1 S^* C^* - \mu S^* - \psi S^* = 0, \tag{9}$$

$$\beta_0 S^* - \beta_1 C^* - (\zeta_1 + \mu + \alpha_1) C = 0, \tag{10}$$

$$\beta_1 S^* - \beta_0 T^* - (\mu + \alpha_2 + \zeta_2) T = 0, \tag{11}$$

$$\beta_0 C^* T^* + \beta_1 T^* C^* - (\mu + \alpha_3 + \zeta_3) B = 0, \tag{12}$$

$$\psi S^* - \theta V^* - \mu V^* = 0, \tag{13}$$

From equation (10), we have

$$C^* = \frac{\beta_0 S^* - (\zeta_1 + \mu + \alpha_1)}{\beta_1} = \Theta_1(S^*), \; say \tag{14}$$

From equation (11), we get

$$T^* = \frac{\beta_1 S^* - (\zeta_2 + \mu + \alpha_2)}{\beta_0} = \Theta_2(S^*), \; say \tag{15}$$

Thus, from equation (12), we get

$$B^* = \frac{(\beta_0 + \beta_1) T^* C^*}{(\zeta_3 + \mu + \alpha_3)} = \frac{(\beta_0 + \beta_1)\, \Theta_1(S^*) \Theta_2(S^*)}{\zeta_3 + \mu + \alpha_3}. \tag{16}$$

From equation (13), we get

$$V^* = \frac{\psi S^*}{\theta + \mu} \tag{17}$$

Using (10), (11), (12) and (13) in equation (9), we have

$$g(S) = A(1-\eta) + \frac{\zeta_1}{\beta_0}\{\beta_1 S^* - (\zeta_2 + \mu + \alpha_2)\} + \frac{\zeta_2}{\beta_1}\{\beta_0 S^* - (\zeta_1 + \mu + \alpha_1)\} + \frac{\zeta_3(\beta_0 + \beta_1)}{(\zeta_3 + \mu + \alpha_3)}$$

$$\left[\left\{\frac{\beta_0 S^* - (\zeta_1 + \mu + \alpha_1)}{\beta_1}\right\}\right]\left[\left\{\frac{\beta_1 S^* - (\zeta_2 + \mu + \alpha_2)}{\beta_0}\right\}\right]$$

$$- \frac{\beta_0 S^*}{\beta_0}\{\beta_1 S^* - (\zeta_2 + \mu + \alpha_2)\} - \frac{\beta_1 S^*}{\beta_1}\{\beta_0 S^* - (\zeta_1 + \mu + \alpha_1)\} - \mu S^* - \psi S^*, \tag{18}$$

$$\therefore g(0) = A(1-\eta) + \frac{\zeta_1}{\beta_0} - (\zeta_2 + \mu + \alpha_2) + \frac{\zeta_2}{\beta_1} - (\zeta_1 + \mu + \alpha_1) + \frac{\zeta_3(\beta_0 + \beta_1)}{\zeta_3 + \mu + \alpha_3}(\zeta_1 + \mu + \alpha_1)$$

$$- \frac{\zeta_3(\beta_0 + \beta_1)}{(\zeta_3 + \mu + \alpha_3)}\left[\left\{\frac{(\zeta_1 + \mu + \alpha_1)(\zeta_2 + \mu + \alpha_2)}{\beta_1 \beta_0}\right\}\right], \tag{19}$$

$$g\left(\frac{A(1-\eta)}{\mu+\psi}\right)=\frac{\zeta_1}{\beta_0}\beta_1\left(\frac{A(1-\eta)}{\mu+\psi}\right)-(\zeta_2+\mu+\alpha_2)+\frac{\zeta_2}{\beta_1}\beta_0\left(\frac{A(1-\eta)}{\mu+\psi}\right)-(\zeta_1+\mu+\alpha_1)$$

$$+\frac{\zeta_3(\beta_0+\beta_1)}{(\zeta_3+\mu+\alpha_3)}\left[\left\{\frac{\beta_0\frac{A(1-\eta)}{\mu+\psi}-(\zeta_1+\mu+\alpha_1)}{\beta_1}\right\}\left\{\frac{\beta_1\frac{A(1-\eta)}{\mu+\psi}-(\zeta_2+\mu+\alpha_2)}{\beta_0}\right\}\right]$$

$$-\beta_1\left(\frac{A(1-\eta)}{\mu+\psi}\right)^2+(\zeta_2+\mu+\alpha_2)\left(\frac{A(1-\eta)}{\mu+\psi}\right)-\beta_0\left(\frac{A(1-\eta)}{\mu+\psi}\right)^2$$

$$+(\zeta_1+\mu+\alpha_1)\left(\frac{A(1-\eta)}{\mu+\psi}\right)-\left(\frac{A(1-\eta)}{\mu+\psi}\right). \tag{20}$$

Using equation (18), we have

$$g^{'}(S)=\frac{\zeta_1\beta_1}{\beta_0}+\frac{\zeta_2\beta_0}{\beta_1}+\frac{\zeta_3(\beta_0+\beta_1)}{(\zeta_3+\mu+\alpha_3)}-2\beta_1S^*+(\zeta_2+\mu+\alpha_2)-2\beta_0S^*+(\zeta_1+\mu+\alpha_1)-\psi-\mu. \tag{21}$$

It can be clearly seen that $g\left(\frac{A(1-\eta)}{\mu+\psi}\right)>0$. Thus, we can conclude that for a given unique value of S^* of x exists if $g(0)<0$ and $g^{'}(S)>0; \forall\, 0<S<\left(\frac{A(1-\eta)}{\mu+\psi}\right)$. So, the corresponding T^*, C^*, B^* and V^* can be obtained from equations (14), (15), (16) and (17) respectively.

5. Basic reproduction number R_0

The basic reproduction number measures the expected values of decreasing or increasing outbreaks of a disease. Using the next generation matrix method R_0 is evaluated as follows:

For the model (1), the disease-free equilibrium point is $E_0\left(\frac{A(1-\eta)}{\mu}, 0, 0, 0, 0\right)$. Decomposing the RHS of the model (1) corresponding to the infected compartments as F_1-F_2. The matrices F_1 and F_2 represent respective new infection and transition matrices, given by

$$F_1=\begin{bmatrix}\beta_0ST-\beta_1TC\\ \beta_1SC-\beta_0zy\\ \beta_0CT+\beta_1TC\\ 0\end{bmatrix} \text{ and } F_2=\begin{bmatrix}(\zeta_1+\mu+\alpha_1)T\\ (\zeta_2+\mu+\alpha_2)C\\ (\zeta_3+\mu+\alpha_3)B\\ (A-\zeta_1y-\zeta_2z-\zeta_3w+\beta_0xy+\beta_1xz+\mu x)\end{bmatrix}$$

Now, we have $X=\left[\frac{dS}{dt}, \frac{dT}{dt}, \frac{dC}{dt}, \frac{dB}{dt}\right]$.

Let us define $\tilde{F_1}=\left[\frac{\partial(R_1)_i}{\partial x_j}\right]$ and $\tilde{F_2}=\left[\frac{\partial(R_2)_i}{\partial x_j}\right]$; for $i, j=1, 2, 3$.

Then, we find

$$\tilde{F_1} = \begin{bmatrix} \beta_0 \dfrac{A(1-\eta)}{\mu+\psi} & 0 & 0 \\ 0 & \beta_1 \dfrac{A(1-\eta)}{\mu+\psi} & 0 \\ 0 & 0 & 0 \end{bmatrix} \text{ and } \tilde{F_2} = \begin{bmatrix} (\zeta_1+\mu+\alpha_1) & 0 & 0 \\ 0 & (\zeta_2+\mu+\alpha_2) & 0 \\ 0 & 0 & (\zeta_3+\mu+\alpha_3) \end{bmatrix}.$$

It then follows that

$$F_1 F_2^{-1} = \begin{bmatrix} \beta_0 \dfrac{A}{\mu} & 0 & 0 \\ 0 & \beta_1 \dfrac{A}{\mu} & 0 \\ 0 & 0 & 0 \end{bmatrix} \begin{bmatrix} \dfrac{1}{\zeta_1+\mu+\alpha_1} & 0 & 0 \\ 0 & \dfrac{1}{\zeta_2+\mu+\alpha_2} & 0 \\ 0 & 0 & \dfrac{1}{\zeta_3+\mu+\alpha_3} \end{bmatrix},$$

i.e.

$$F_1 F_2^{-1} = \begin{bmatrix} \dfrac{\beta_0 A(1-\eta)}{(\mu+\psi)(\zeta_1+\mu+\alpha_1)} & 0 & 0 \\ 0 & \dfrac{\beta_1 A(1-\eta)}{(\mu+\psi)(\zeta_2+\mu+\alpha_2)} & 0 \\ 0 & 0 & 0 \end{bmatrix}. \tag{22}$$

Therefore, we have

$$R_0 = max\left[\beta_0 \frac{A(1-\eta)}{(\mu+\psi)(\zeta_1+\mu+\alpha_1)},\ \beta_1 \frac{A(1-\eta)}{(\mu+\psi)(\zeta_2+\mu+\alpha_2)},\ 0\right]. \tag{23}$$

As the propagation rate of TB is substantially lower than the propagation rate of COVID-19 infection. Therefore, the basic reproduction number for the model is given by

$$R_0 = \frac{\beta_1 A(1-\eta)}{(\mu+\psi)(\zeta_2+\mu+\alpha_2)}. \tag{24}$$

Thus, COVID-19 infection rate contributes to the basic reproduction number in the case of the coinfection diseases TB and COVID-19.

6. Stability analysis of equilibrium points

Here, we discuss only the local stability of the two equilibrium points.

6.1 *Local stability of disease free equilibrium point*

When a critical point is locally stable, the system will eventually move to the same point regardless of where it is initially set. Now, we will discuss the local stability by using the following computed Variational matrix:

$$V(E) = \begin{bmatrix} g_{11} & g_{12} & g_{13} & 0 & 0 \\ g_{21} & g_{22} & g_{23} & 0 & 0 \\ g_{31} & g_{32} & g_{33} & 0 & 0 \\ 0 & g_{42} & g_{43} & g_{44} & 0 \\ g_{51} & 0 & 0 & 0 & g_{55} \end{bmatrix}$$

where $g_{11} = -\beta_0 T - \beta_1 C - \mu - \psi$, $g_{12} = \zeta_1 - \beta_0 S$, $g_{13} = \zeta_2 - \beta_1 S$, $g_{21} = \beta_0 T$, $g_{22} = \beta_0 S - \beta_1 C - (\zeta_1 + \mu + \alpha_1)$, $g_{23} = -\beta_1 T$, $g_{31} = \beta_1 C$, $g_{32} = -\beta_0 C$, $g_{33} = \beta_1 S - \beta_0 T - (\mu + \alpha_2 + \zeta_2)$, $g_{42} = \beta_0 C + \beta_1 C$, $g_{43} = \beta_1 T + \beta_0 T$, $g_{44} = -(\mu + \alpha_3 + \zeta_3)$, $g_{51} = \psi$, $g_{55} = -(\theta + V)$.

The variational matrix $V(E_0)$ at disease free equilibrium point is given by

$$V(E_0) = \begin{bmatrix} g_{11} & g_{12} & g_{13} & 0 & 0 \\ 0 & a_{22} & 0 & 0 & 0 \\ 0 & 0 & g_{33} & 0 & 0 \\ 0 & 0 & 0 & g_{44} & 0 \\ g_{51} & 0 & 0 & 0 & g_{55} \end{bmatrix}$$

where $g_{11} = -\mu - \psi$, $g_{12} = \zeta_1 - \beta_0 \dfrac{A(1-\eta)}{\mu}$, $g_{13} = \zeta_2 - \beta_1 \dfrac{A(1-\eta)}{\mu}$, $g_{22} = \beta_0 \frac{A(1-\eta)}{\mu} - (\zeta_1 + \mu + \alpha_1)$, $g_{33} = -\beta_1 \dfrac{A(1-\eta)}{\mu} - (\mu + \alpha_2 + \zeta_2)$, $g_{44} = -(\mu + \alpha_3 + \zeta_3)$, $g_{51} = \psi$, $g_{55} = -(\theta + V)$.

The eigenvalues of the disease free equillibrium corresponding to variational matrix are given below:

$\lambda_1 = -(\theta + V)$,

$\lambda_2 = -(\zeta_3 + \mu + \alpha_3)$,

$\lambda_3 = -(\mu + \psi)$,

$\lambda_4 = -(\zeta_1 + \mu + \alpha_1)(1 - R_1)$,

$\lambda_5 = (\mu + \alpha_2 + \zeta_2)(1 - R_2)$.

Clearly, it can be seen that the three eigenvalues λ_1, λ_2 and λ_3 of the above variational matrix are found to be negative for the DFE point and the rest two eigenvalues λ_4 and λ_5 have negative real parts. Thus, using Routh-Hurwitz criterion, the DFE point is **locally asymptotically stable**, if $R_1 < 1$, $R_2 < 1$ and **unstable** if $R_1 > 1$, $R_2 > 1$ [37].

6.2 *Local stability of endemic equilibrium point*

To determine the local stability of endemic equilibrium point P^*, the system is linearized about endemic equilibrium point by setting $S = S_1 + S^*$, $T = T_1 + T^*$, $C = C_1 + C^*$, $B = B_1 + B^*$ and $V = V_1 + V^*$. After linearization, equation (1) can be written as follows:

$$\frac{dS_1}{dt} = \zeta T_1 + \zeta_2 C_1 + \zeta_3 B_1 - \beta_0 S_1 T^* - \beta_0 S^* T_1 - \beta_1 S^* C_1 - \beta_1 S_1 C^* - \mu S_1 - \psi S,$$

$$\frac{dT_1}{dt} = \beta_0 S^* T_1 + \beta_0 S_1 T^* - \beta_1 T_1 C^* - \beta_1 T^* C_1 - (\mu + \alpha_1 + \zeta_1) T_1,$$

$$\frac{dC_1}{dt} = \beta_1 S^* C_1 + \beta_1 S_1 C^* - \beta_0 C^* T_1 - \beta_0 C_1 T^* - (\mu + \alpha_2 + \zeta_2) C_1,$$

$$\frac{dB_1}{dt} = \beta_0 C^* T_1 + \beta_0 C_1 T^* + \beta_1 T^* C_1 + \beta_1 T_1 C^* - (\mu + \alpha_3 + \zeta_3) B_1,$$

$$\frac{dV_1}{dt} = \psi S^* + \psi S^* - \theta V^* - \theta V_1 - \mu V^* - \mu V_1.$$

Now, let us consider the following Lyapunov function:

$$L_1 = \frac{1}{2} S_1^2 + \frac{1}{2} T_1^2 + \frac{1}{2} C_1^2 + \frac{1}{2} B_1^2 + \frac{1}{2} V_1^2. \tag{25}$$

Differentiating (25) w.r.t. t, we have

$$\begin{aligned}
\dot{L_1} = & -\frac{1}{4} g_{11} S_1^2 + g_{12} S_1 T_1 - \frac{1}{3} g_{22} T_1^2, \\
& -\frac{1}{4} g_{11} S_1^2 + g_{13} S_1 C_1 - \frac{1}{3} g_{33} C_1^2, \\
& -\frac{1}{4} g_{11} S_1^2 + g_{14} S_1 B_1 - \frac{1}{3} g_{44} B_1^2, \\
& -\frac{1}{4} g_{11} S_1^2, -g_{15} S_1^2 V_1 - g_{55} V_1^2, \\
& -\frac{1}{3} g_{22} T_1^2 + g_{24} T_1 B_1 - \frac{1}{3} g_{44} B_1^2, \\
& -\frac{1}{3} g_{33} C_1^2 + g_{34} C_1 B_1 - \frac{1}{3} g_{44} B_1^2, \\
& -\frac{1}{3} g_{22} T_1^2 + g_{23} T_1 C_1 - \frac{1}{3} g_{33} C_1^2.
\end{aligned}$$

where

$$g_{11} = (-\beta_0 T^* - \beta_1 C^* - \mu),\ g_{22} = \{\beta_0 S^* - \beta_1 C^* - (\zeta_1 + \mu + \alpha_1)\},\ g_{33} = \{\beta_1 S^* - \beta_0 T^* - (\mu + \alpha_2 + \zeta_2)\},$$

$$g_{44} = \{-(\mu + \alpha_3 + \zeta_3)\},\ g_{55} = \{-(\theta V)\},\ g_{12} = \{\zeta_1 - \beta_0 S^* + \beta_0 T^*\},\ g_{13} = \{\zeta_2 - \beta_1 S^* + \beta_1 C^*\},$$

$$g_{14} = \zeta_3,\ g_{15} = \psi,\ g_{23} = \{-\beta_1 T^* - \beta_0 C^*\},\ g_{24} = \{\beta_0 C^* + \beta_1 C^*\},\ g_{34} = \{\beta_0 T^* + \beta_1 T^*\},$$

The Lyapunov function $\dot{L}_1$ is negative definite, if the following conditions hold:

$$(i) \quad (\zeta_1 - \beta_0 S^* + \beta_0 T^*)^2 < \frac{1}{3}(-\beta_0 T^* - \beta_1 C^* - \mu)\{\beta_0 S^* - \beta_1 C^* - (\zeta_1 + \mu + \alpha_1)\},$$

$$(ii) \quad (\zeta_2 - \beta_1 S^* + \beta_1 C^*)^2 < \frac{1}{3}(-\beta_0 T^* - \beta_1 C^* - \mu)\{\beta_1 S^* - \beta_0 C^* - (\zeta_2 + \mu + \alpha_2)\},$$

$$(iii) \quad \zeta_3^2 < \frac{1}{3}(-\beta_0 T^* - \beta_1 C^* - \mu)\{-(\mu + \alpha_3 + \zeta_3)\},$$

$$(iv) \quad \psi^2 < (-\beta_0 T^* - \beta_1 C^* - \mu)\{-(\theta V)\},$$

$$(v) \quad (\beta_1 T^* + \beta_0 C^*)^2 < \frac{4}{9}\{\beta_0 S^* - \beta_1 C^*(\zeta_1 + \mu + \alpha_1)\}\{+\beta_1 S^* - \beta_0 T^* - (\mu + \alpha_2 + \zeta_2)\},$$

$$(vi) \quad (\beta_0 + \beta_1)^2 C^{*2} < \frac{4}{9}\{\beta_0 S^* - \beta_1 C^* - (\zeta_1 + \mu + \alpha_1)\}\{-(\zeta_3 + \mu + \alpha_3)\},$$

$$(vii) \quad (\beta_0 + \beta_1)^2 T^{*2} < \frac{4}{9}\{\beta_1 S^* - \beta_0 T^* - (\zeta_2 + \mu + \alpha_2)\}\{-(\zeta_3 + \mu + \alpha_3)\}.$$

Thus, if all the conditions from (i)-(vii) are satisfied, then the endemic equilibrium point P^* is **locally asymptotically stable**.

6.3 *Global stability of endemic equilibrium point*

Here, we discuss the global stability of the endemic equilibrium point $P^*(S^*, T^*, C^*, B^*, V^*)$, which is given in the form of theorem as follows:

Theorem 4.6.3.1 The endemic equilibrium point $P^*(S^*, T^*, C^*, B^*, V^*)$ is globally asymptotically stable, if the Lyapunov function

$$L_2 = \frac{1}{2}\left\{(S - S^*)^2 + (T - T^*)^2 + (C - C^*)^2 + (B - B^*)^2 + (V - V^*)^2\right\}$$

satisfies the conditions given in proof of this theorem:

Proof. Consider the following Lyapunov function

$$L_2 = \frac{1}{2}\left\{(S-S^*)^2 + (T-T^*)^2 + (C-C^*)^2 + (B-B^*)^2 + (V-V^*)^2\right\}$$

Let $L_2 \geq 0$ at the endemic equilibrium point, and S, T, C, B, and V respectively represent the transformed susceptible individuals, transformed TB infected individuals, transformed COVID-19 infected individuals, transformed TB plus COVID-19 infected individuals, and transformed vaccinated individuals. Differentiating the function L_2 w.r.t. t we get

$$\begin{aligned}
\dot{L_2} &= (S-S^*)\dot{S} + (T-T^*)\dot{T} + (C-C^*)\dot{C} + (B-B^*)\dot{B} + (V-V^*)\dot{V} \\
&= -\frac{1}{4}b_{11}(S-S^*)^2 + b_{12}(S-S^*)(T-T^*) - \frac{1}{3}b_{22}(T-T^*)^2, \\
&\quad -\frac{1}{4}b_{11}(S-S^*)^2 + b_{13}(S-S^*)(C-C^*) - \frac{1}{3}b_{33}(C-C^*)^2, \\
&\quad -\frac{1}{4}b_{11}(S-S^*)^2 + b_{14}(S-S^*)(B-B^*) - \frac{1}{3}b_{44}(B-B^*)^2, \\
&\quad -\frac{1}{4}b_{11}(S-S^*)^2 + b_{15}(S-S^*)(V-V^*) - b_{55}(V-V^*)^2, \\
&\quad -\frac{1}{3}b_{22}(T-T^*)^2 + b_{13}(T-T^*)(C-C^*) - \frac{1}{3}b_{33}(C-C^*)^2, \\
&\quad -\frac{1}{3}b_{22}(T-T^*)^2 + b_{24}(T-T^*)(B-B^*) - \frac{1}{3}b_{44}(B-B^*)^2, \\
&\quad -\frac{1}{3}b_{33}(C-C^*)^2 + b_{34}(C-C^*)(B-B^*) - \frac{1}{3}b_{44}(B-B^*)^2.
\end{aligned}$$

$$b_{11} = -\left\{-\beta_0 T^* + \beta_1 C^* + \mu + \psi\right\},\ b_{22} - \left\{\beta_0 S^* + \beta_1 C^* + (\zeta_1 + \mu + \alpha_1)\right\},\ b_{12} = \zeta_1 - \beta_0 S^* + \beta_0 T^*,$$

$$b_{44} = -\mu + \alpha_3 + \zeta_3,\ b_{55} = -\theta,\ b_{33} = -\left\{-\beta_1 S^* + \beta_0 T^* + (\mu + \alpha_2 + \zeta_2)\right\},\ b_{13} = \zeta_2 - \beta_1 S^* + \beta_1 C^*,$$

$$b_{14} = \zeta_3,\ b_{15} = \psi,\ b_{23} = -\beta_1 T^* - \beta_0 C^*,\ b_{24} = \beta_0 C^*,\ b_{34} = \beta_0 T^* + \beta_1 T^*.$$

The Lyapunov function $\dot{L_2}$ is negative definite, if the following conditions hold:

$$b_{12}^2 < \frac{1}{3}b_{11}b_{22},\ b_{13}^2 < \frac{1}{3}b_{11}b_{33},\ b_{14}^2 < \frac{1}{3}b_{11}b_{44},\ b_{15}^2 < \frac{1}{3}b_{11}b_{55},$$

$$b_{23}^2 < \frac{1}{3}b_{22}b_{33},\ b_{24}^2 < \frac{1}{3}b_{22}b_{44},\ b_{34}^2 < \frac{1}{3}b_{33}b_{44}.$$

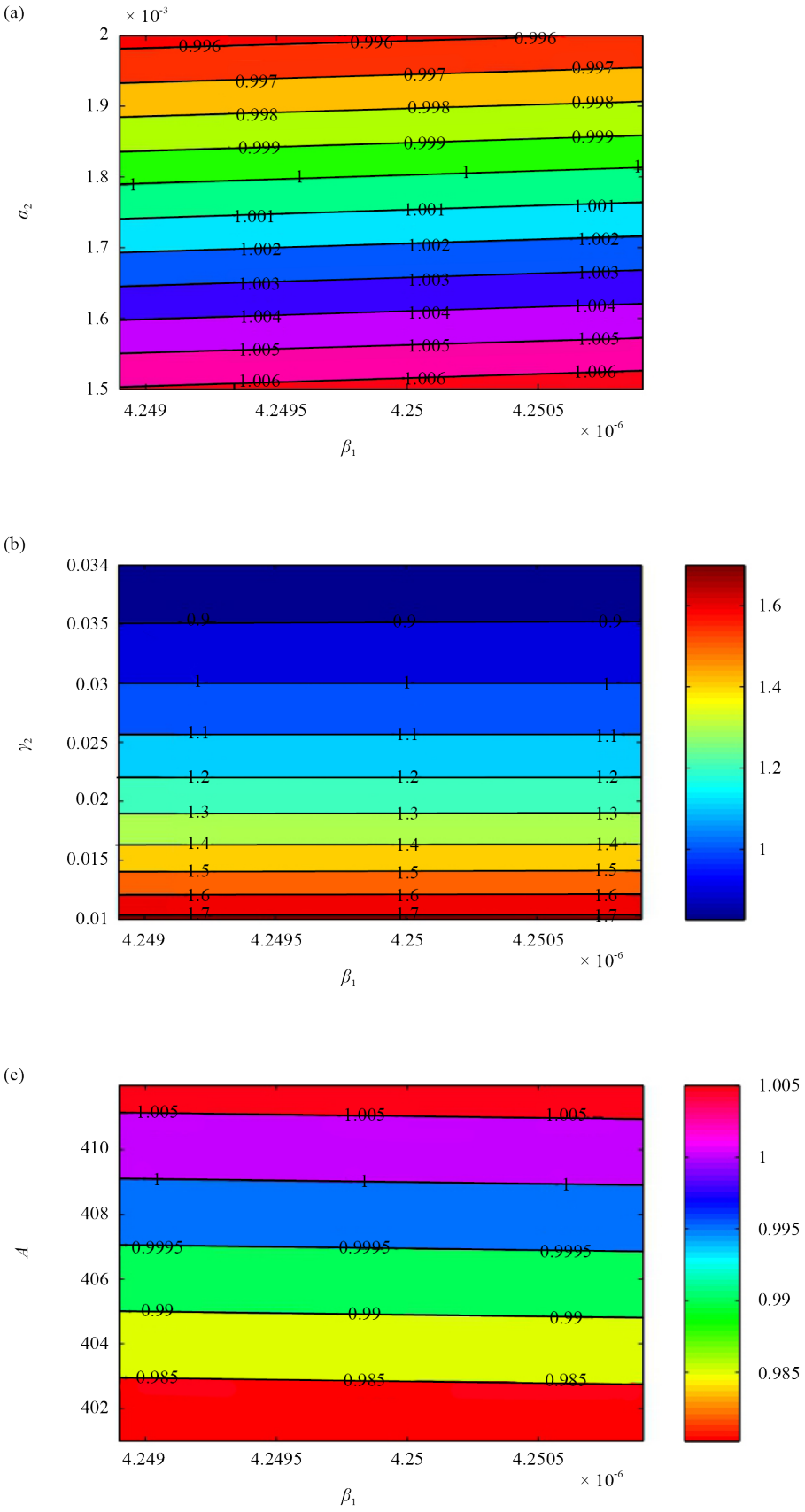
(a)
× 10^-3
2
1.9
1.8
1.7
1.6
1.5
α2
0.996
0.997
0.998
0.999
1
1.001
1.002
1.003
1.004
1.005
1.006
4.249
4.2495
4.25
4.2505
× 10^-6
β1
(b)
0.034
0.035
0.03
0.025
0.02
0.015
0.01
γ2
0.9
1
1.1
1.2
1.3
1.4
1.5
1.6
1.7
4.249
4.2495
4.25
4.2505
× 10^-6
β1
1.6
1.4
1.2
1
(c)
410
408
406
404
402
A
1.005
1
0.9995
0.99
0.985
4.249
4.2495
4.25
4.2505
× 10^-6
β1
1.005
1
0.995
0.99
0.985

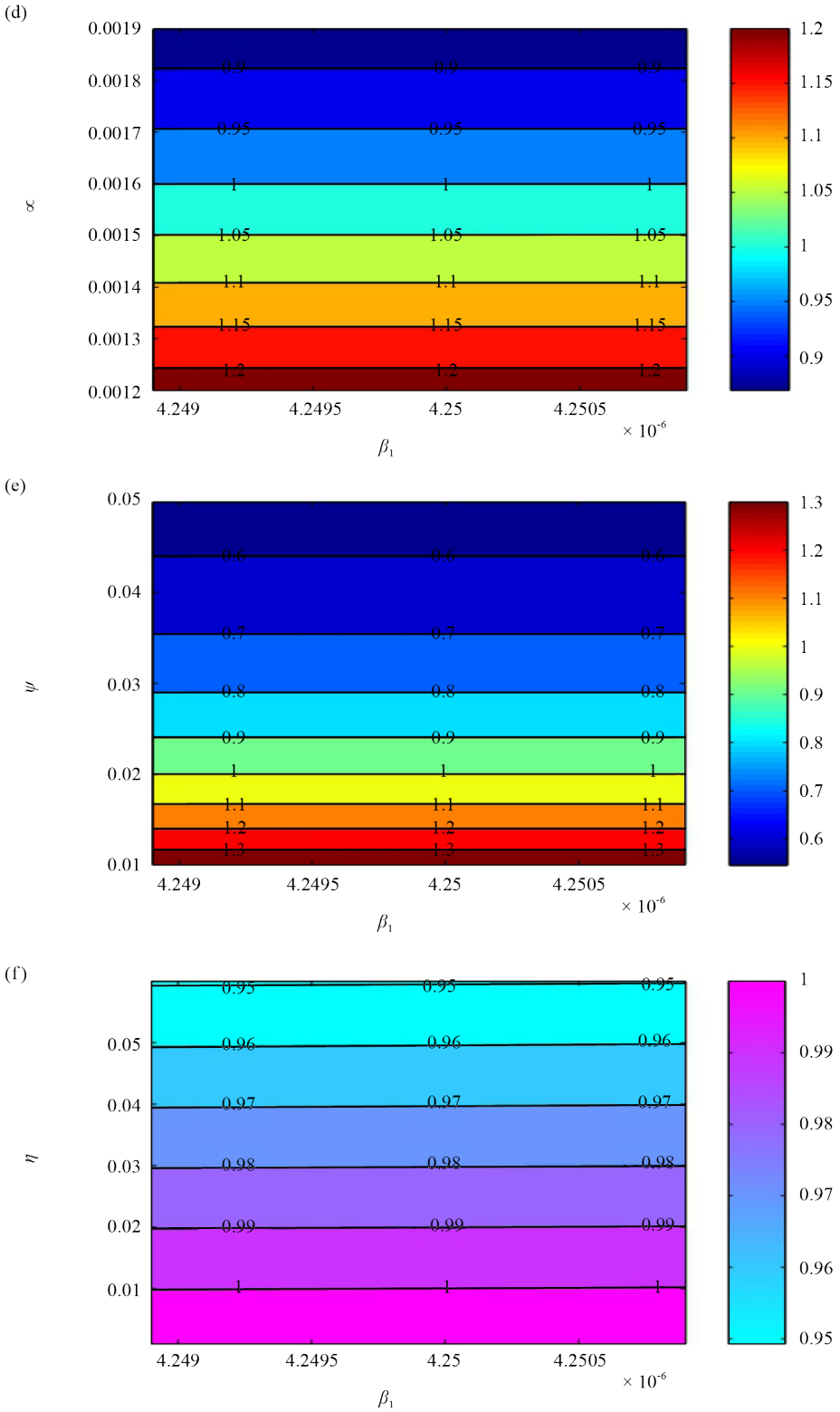

Figure 2. Matrix plots showing the changing nature in basic reproduction number (R_0) of STCBV model under parametric variations: (a) R_0 vs (β_1, α_2) $\in [4.2489 \times 10^{-6}, 4.2509 \times 10^{-6}] \times [0.02, 0.1]$, (b) R_0 vs (β_1, ζ_2) $\in [4.2489 \times 10^{-6}, 4.2509 \times 10^{-6}] \times [0.02, 0.06]$, (c) R_0 vs (β_1, A) $\in [4.2489 \times 10^{-6}, 4.2509 \times 10^{-6}] \times [402, 410]$, (d) R_0 vs (β_1, μ) $\in [4.2489 \times 10^{-6}, 4.2509 \times 10^{-6}] \times [0.012, 0.019]$, (e) R_0 vs (β_1, ψ) $\in [4.2489 \times 10^{-6}, 4.2509 \times 10^{-6}] \times [0.02, 0.05]$, (f) R_0 vs (β_1, η) $\in [4.2489 \times 10^{-6}, 4.2509 \times 10^{-6}] \times [0.01, 0.05]$

Hence, if the above conditios are satisfied then the endemic equilibrium point P^* is **globally asymptotically stable**. The impact of parameter variation R_0 is further investigated under $\beta_1 \times \alpha_2 \in [0.0000042489, 0.0000042509] \times [0.02, 0.1]$, $\beta_1 \times \gamma_2 \in [0.0000042489, 0.0000042509] \times [0.02, 0.06]$, $\beta_1 \times A \in [0.0000042489, 0.0000042509] \times [402, 410]$, $\beta_1 \times \mu \in [0.0000042489, 0.0000042509] \times [0.012, 0.019]$, $\beta_1 \times \psi \in [0.0000042489, 0.0000042509] \times [0.02, 0.05]$ and $\beta_1 \times \eta \in [0.0000042489, 0.0000042509] \times [0.01, 0.05]$ in Figure 2. It is also seen that only the increasing value of β_1 can shift $R_0 < 1$ to $R_1 > 1$ in Figure 2(a). Further, the simultaneously increasing value increase the value of R_0 in Figure 2(b, c, d, e, f).

7. Sensitivity analysis

In the model (1), seven biological parameters have been used which are β, A, η, μ, ζ_2, α_2 and ψ, which affect the basic reproduction number R_0. The partial derivative given below represents R_0's sensitivity to changes in various biological parameters.

The sensitivity of any parameter 'H' w.r.t. R_0 is defined as how the model behaves to a small change in H according to the following definition:

$$K_H = \frac{\partial R_0}{\partial H}\frac{H}{R_0}$$

where

$$R_0 = \frac{\beta_1 A(1-\eta)}{(\mu+\psi)(\zeta_2+\mu+\alpha_2)}.$$

The various sensitivity indices with regard to R_0 for the model parameters are given below:

$$\left.\begin{aligned} &K_{\beta_1} = \frac{\partial R_0}{\partial \beta_1}\frac{\beta_1}{R_0} = 1,\ K_\Lambda = \frac{\partial R_0}{\partial \Lambda}\frac{\Lambda}{R_0} = 1,\ K_\eta = \frac{\partial R_0}{\partial \eta}\frac{\eta}{R_0} = -0.01,\\ &K_\mu = \frac{\partial R_0}{\partial \mu}\frac{\mu}{R_0} = -0.77,\ K_{\zeta_2} = \frac{\partial R_0}{\partial \zeta_2}\frac{\zeta_2}{R_0} = -0.62,\\ &K_{\alpha_2} = \partial R_0 \partial \alpha_2 \frac{\alpha_2}{R_0} = -0.0018,\ K_\mu = \frac{\partial R_0}{\partial \mu}\frac{\mu}{R_0} = -0.77. \end{aligned}\right\}$$

In Figure 3, a grraphical representation of sensitivity indices for model parameters w.r.t. R_0 is shown and on the basis of this plot, it is revealed that β and A have high positive impact on the spread of the diseases and other model parameters have negative impact.

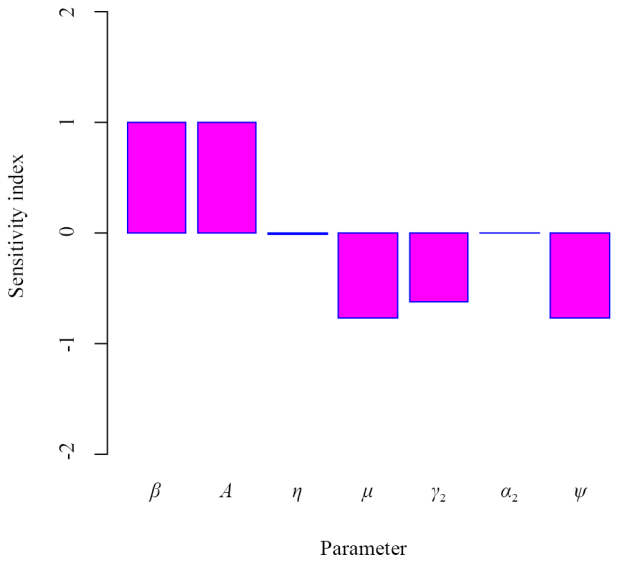

Figure 3. Sensitivity analysis of parameters

8. Numerical simulation

The TB-COVID-19 coinfection model is numerically solved. Table 2 gives the model parameter values which are used to perform numerical simulation of the model by using mathematical softwares MATLAB and Mathematica. Most of parameter values have been taken from available literature and some of them are fitted or estimated. Now various graphs are plotted to interpret the findings.

Table 2. Description of parameters for TB-COVID-19 model

Parameter	Value	Source
A	408.99 day^{-1}	Estimated
α_1	0.004 day^{-1}	[38]
α_2	0.0018 day^{-1}	[38]
α_3	0.007 day^{-1}	Estimated
β_0	2×10^{-6}	[38]
β_1	5.5×10^{-6}	[38]
ζ_1	0.00035 day^{-1}	Estimated
ζ_2	0.03 day^{-1}	Assumed
ζ_3	0.01 day^{-1}	Estimated
μ	0.016 day^{-1}	Estimated
ψ	0.02 day^{-1}	Fitted
θ	0.004 day^{-1}	Estimated
η	0.01 day^{-1}	Fitted

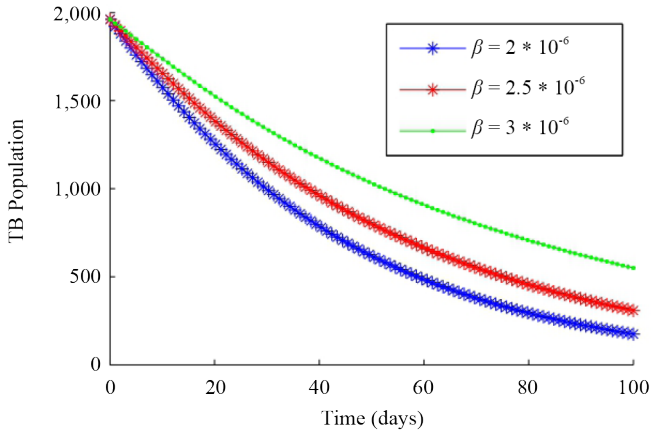

Figure 4. Fluctuation in TB prevalence with varying β

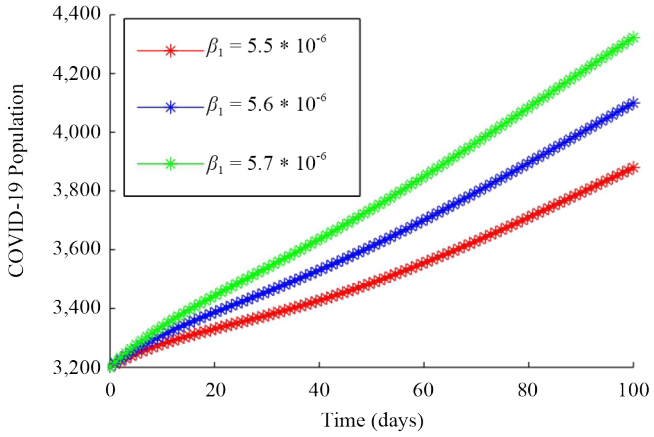

Figure 5. Fluctuation in COVID-19 incidence with time for different values of β_1

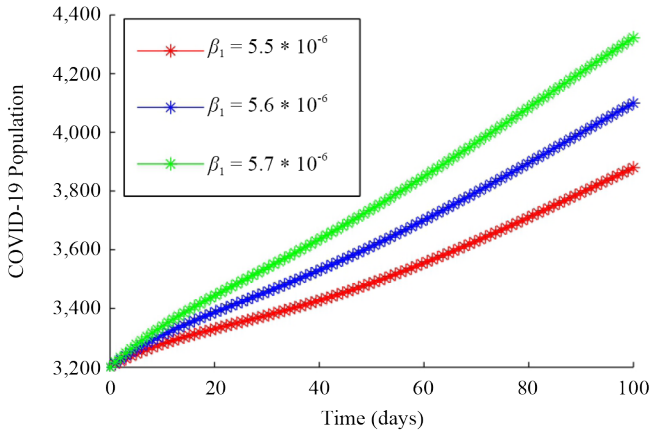

Figure 6. Combined prevalence variations of TB & COVID-19 with time for different values of β_1

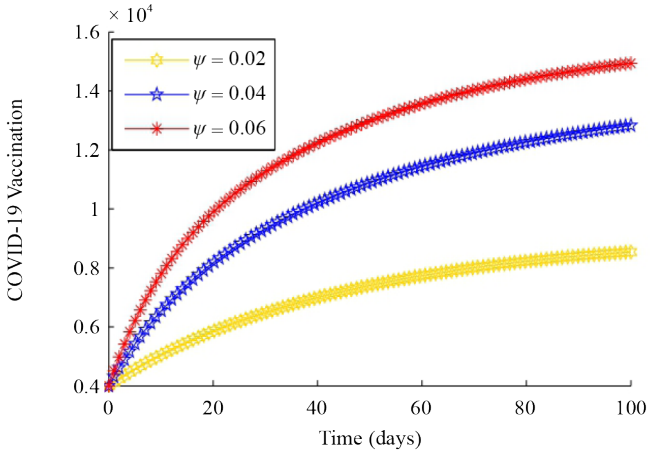

Figure 7. Variation of COVID-19 vaccinated patients with time for different values of ψ

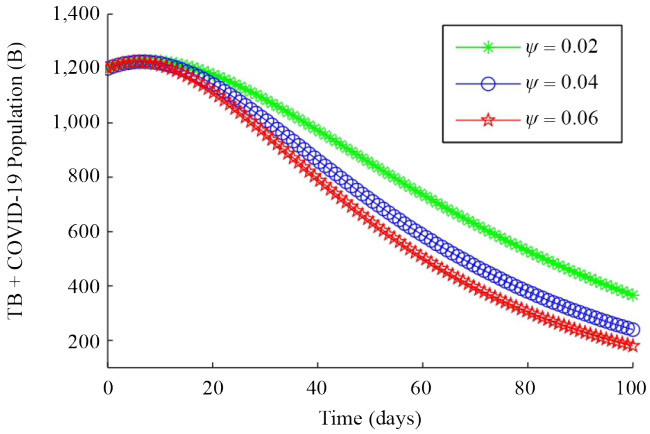

Figure 8. Variation of TB & COVID-19 patients with time for different values of ψ

In Figure 4, we have shown how the population infected with TB population changes over time in the context of COVID-19 infection. From the figure we have noticed a significant reduction in the reported cases of tuberculosis infection. This decline in the number of TB-infected individuals could possibly be attributed to instances where TB is misdiagnosed as COVID-19 resulting in TB patients being treated as if they were infected with COVID-19. In Figure 5, we have drawn the variation of COVID-19 infected population with time for different values of β_1. From this figure, we observe observe that the increasing value of transimission coefficient increases the number of COVID-19 infected population which implies as the infection rate will increase the number of infected population of COVID-19 will also increase. In Figure 6, we have drawn the variation of TB & COVID-19 population with time for different values of β_1. Observations indicate that an increase in the value of β_1 corresponds to a decrease in the number of coinfected TB plus COVID-19 population. This suggests that COVID-19 has had a severe impact on the TB population, leading to a decline caused by inadequate healthcare, misdiagnosis, and the similarity in symptoms between COVID-19 and TB, resulting in TB patients being treated as if they have COVID-19. In Figure 7, we have shown the variation of COVID-19 vaccinated population with time for different values of ψ. From this figure, it is observed that as the vaccination rate ψ of COVID-19 increases, the vaccination coverage also increases which will definetly help in controlling the disease. From Figure 8, it is observed that the disease (TB plus COVID-19) trajectory below all others is the one with the highest vaccination coverage 0.06. High vaccination rates thereby prevent the disease from spreading but do not completely eradicate it. Therefore,

the vaccination approach for disease control needs to be improved in terms of immunizing people at very young ages to combat the initial infectious peak.

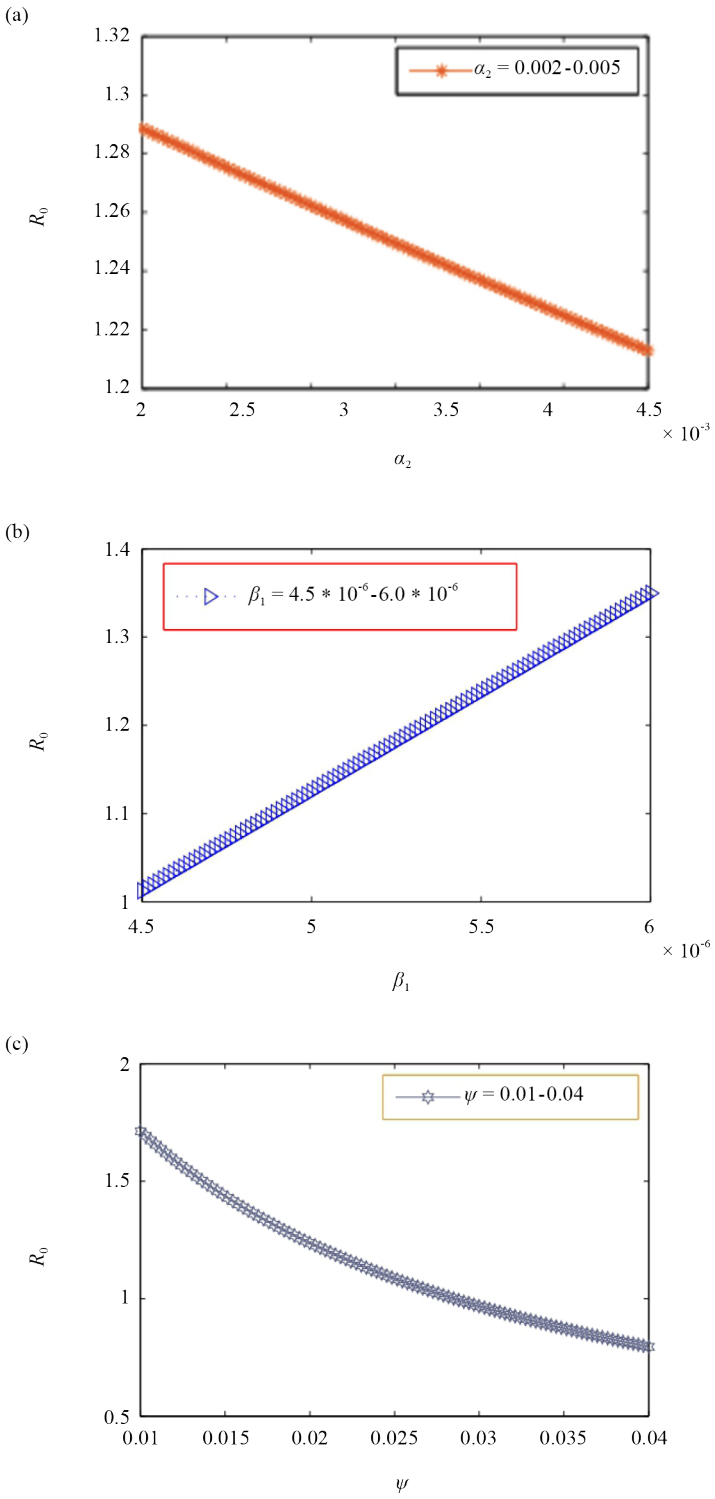

Figure 9. Fluctuation of R_0 with α_2, β_1 and ψ

Figure 9, shows the fluctuation in R_0 with parameters α_2, β_1 and ψ. From the Figures 9(a) and 9(b), R_0 can be seen increasing linearly for both, the propagation rate β_1 of COVID-19 infection. However, it is observed that R_0 decreases exponentially and approaches to zero as the vaccination rate ψ of COVID-19 vaccination increases.

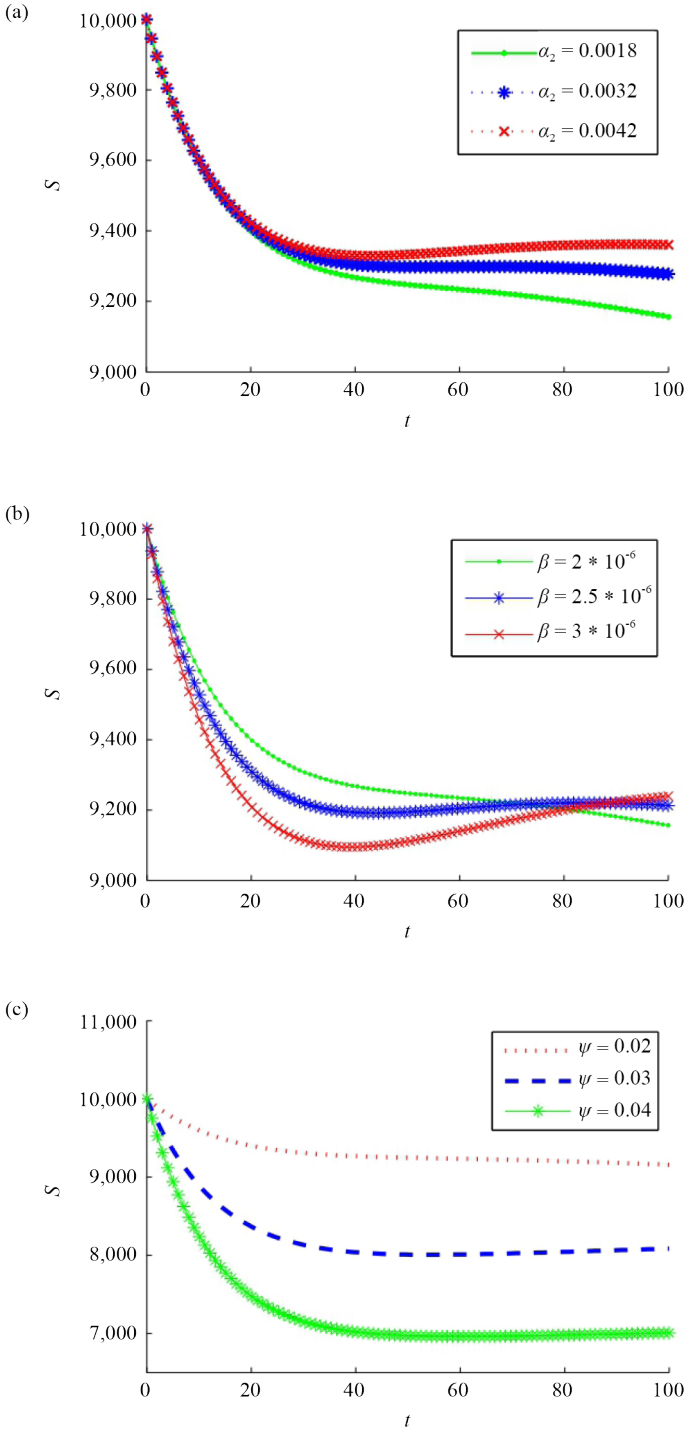

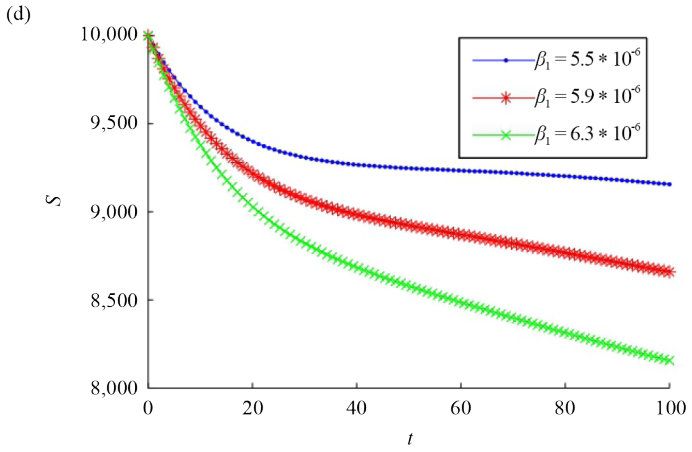

Figure 10. Variaton of susceptible population with time t for different values of α_2, β, ψ and β_1

In Figure 10, we have shown the effects of α_2, β, ψ and β_1 on S. Figure 10(a) demonstrates the variation of the susceptible population in relation to the COVID-19 infection population with the death rate α_2 due to disease. Figure 10(b) demonstrates that as we increase the infection rate β of TB the number of susceptibles population decreases. Figure 10(c) indicates that the vaccination has a large effect on the susceptible population as the susceptible population grows and the mass vaccination program (i.e. vaccination rate ψ) expands. Figure 10(d) shows that as we increase the infection rate β of COVID-19 the number of susceptible population decreases. In Figure 2, the different matrix plots are shown. From this figure it can be seen that μ, ζ_2 and ψ are negatively correlated, and β, A, η and α_2 are positively correlated to R_0.

9. Conclusion

In this paper, the disease dynamics of COVID-19 and tuberculosis co-infection is formulated and analysed. The basic properties such as positivity and boundedness have been established. The equilibrium points are searched and disease free & endemic equilibrium points are found to exist. In this paper, an epidemiological model is proposed to study the dynamics of coinfection diseases (TB) and COVID-19 with the effect of vaccination. Tuberculosis (TB) and COVID-19 both are infectious diseases that pose significant global health challenges. Evidence suggests that individuals with TB have a higher risk of acquiring the COVID-19 infection. With the emergence of the COVID-19 pandemic, concerns have arisen regarding the potential impact of the concomitant presence of TB and COVID-19.

Acknowledgments

I would like to thank Abhishekh Singh and Manik sen for their constant support and encouragement.

Conflict of interest

The author declares no competing financial interest

References

[1] Georgiev S. Mathematical identification analysis of a fractional-order delayed model for tuberculosis. *Fractal and Fractional*. 2023; 7(7): 538.

[2] Adhikari SP, Meng S, Wu YJ, Mao YP, Ye RX, Wang QZ, et al. Epidemiology, causes, clinical manifestation and diagnosis, prevention and control of coronavirus disease (COVID-19) during the early outbreak period: a scoping review. *Infectious Diseases of Poverty*. 2020; 9(1): 1-2.

[3] Wang C, Horby PW, Hayden FG, Gao GF. A novel coronavirus outbreak of global health concern. *The Lancet*. 2020; 395(10223): 470-473.

[4] Laxminarayan R, Wahl B, Dudala SR, Gopal K, Mohan BC, Neelima S, et al. Epidemiology and transmission dynamics of COVID-19 in two Indian states. *Science*. 2020; 370(6517): 691-697.

[5] Spelta A, Flori A, Pierri F, Bonaccorsi G, Pammolli F. After the lockdown: simulating mobility, public health and economic recovery scenarios. *Scientific Reports*. 2020; 10(1): 16950.

[6] Saha J, Chouhan P. Lockdown and unlock for the COVID-19 pandemic and associated residential mobility in India. *International Journal of Infectious Diseases*. 2021; 104: 382-389.

[7] Acharya R, Porwal A. A vulnerability index for the management of and response to the COVID-19 epidemic in India: an ecological study. *The Lancet Global Health*. 2020; 8(9): 1142-1151.

[8] Das P, Upadhyay RK, Misra AK, Rihan FA, Das P, Ghosh D. Mathematical model of COVID-19 with comorbidity and controlling using non-pharmaceutical interventions and vaccination. *Nonlinear Dynamics*. 2021; 106(2): 1213-1227.

[9] Acuña Zegarra MA, Díaz Infante S, Baca Carrasco D, Olmos Liceaga D. COVID-19 optimal vaccination policies: A modeling study on efficacy, natural and vaccine-induced immunity responses. *Mathematical Biosciences*. 2021; 337: 108614.

[10] Guan WJ, Liang WH, Zhao Y, Liang HR, Chen ZS, Li YM, et al. Comorbidity and its impact on 1590 patients with COVID-19 in China: a nationwide analysis. *European Respiratory Journal*. 2020; 55(5): 2000547.

[11] Sharma N, Singh R, Pathak R. Modeling of media impact with stability analysis and optimal solution of SEIRS epidemic model. *Journal of Interdisciplinary Mathematics*. 2019; 22(7): 1123-1156.

[12] Asamoah JK, Jin Z, Sun GQ, Seidu B, Yankson E, Abidemi A, et al. Sensitivity assessment and optimal economic evaluation of a new COVID-19 compartmental epidemic model with control interventions. *Chaos, Solitons & Fractals*. 2021; 146: 110885.

[13] Chen Y, Wang Y, Fleming J, Yu Y, Gu Y, Liu C, et al. Active or latent tuberculosis increases susceptibility to COVID-19 and disease severity. *MedRxiv*. 2020; 16: 1-15. Available from: https://doi.org/10.1101/2020.03.10.20033795.

[14] Ul Rehman A, Singh R, Singh J. Mathematical analysis of multi-compartmental malaria transmission model with reinfection. *Chaos, Solitons & Fractals*. 2022; 163: 112527.

[15] Li Q, Guan X, Wu P, Wang X, Zhou L, Tong Y, et al. Early transmission dynamics in Wuhan, China, of novel coronavirus-infected pneumonia. *New England Journal of Medicine*. 2020; 382(13): 1199-1207.

[16] Marimuthu Y, Nagappa B, Sharma N, Basu S, Chopra KK. COVID-19 and tuberculosis: A mathematical model based forecasting in Delhi, India. *Indian Journal of Tuberculosis*. 2020; 67(2): 177-181.

[17] Walaza S, Cohen C, Tempia S, Moyes J, Nguweneza A, Madhi SA, et al. Influenza and tuberculosis co-infection: A systematic review. *Influenza and Other Respiratory Viruses*. 2020; 14(1): 77-91.

[18] Gupta D. Conscientious objections during COVID-19 pandemic. *Indian Journal of Community Health*. 2020; 32(2): 231-235.

[19] Chadha VK. Tuberculosis epidemiology in India: a review. *The International Journal of Tuberculosis and Lung Disease*. 2005; 9(10): 1072-1082.

[20] Singh R, Ul Rehman A, Ahmed T, Ahmad K, Mahajan S, Pandit AK, et al. Mathematical modelling and analysis of COVID-19 and tuberculosis transmission dynamics. *Informatics in Medicine Unlocked*. 2023; 38: 101235.

[21] Nkamba LN, Manga TT, Agouanet F, Mann Manyombe ML. Mathematical model to assess vaccination and effective contact rate impact in the spread of tuberculosis. *Journal of Biological Dynamics*. 2019; 13(1): 26-42.

[22] Kumar P, Vellappandi M, Khan ZA, Sivalingam SM, Kaziboni A, Govindaraj V. A case study of monkeypox disease in the United States using mathematical modeling with real data. *Mathematics and Computers in Simulation*. 2023; 13(1): 26-42.

[23] Sivalingam SM, Govindaraj V. A novel numerical approach for time-varying impulsive fractional differential equations using theory of functional connections and neural network. *Expert Systems with Applications*. 2023; 13(1): 121750.

[24] Kumar P, Govindaraj V. A novel optimization-based physics-informed neural network scheme for solving fractional differential equations. *Engineering with Computers*. 2023; 1(2): 855-865.

[25] Yang J, Zheng YA, Gou X, Pu K, Chen Z, Guo Q, et al. Prevalence of comorbidities and its effects in patients infected with SARS-CoV-2: a systematic review and meta-analysis. *International Journal of Infectious Diseases*. 2020; 94: 91-95.

[26] Guan WJ, Liang WH, Zhao Y, Liang HR, Chen ZS, Li YM, et al. Comorbidity and its impact on 1590 patients with COVID-19 in China: a nationwide analysis. *European Respiratory Journal*. 2020; 55(5): 2000547.

[27] Carreira H, Strongman H, Peppa M, McDonald HI, Dos Santos Silva I, Stanway S, et al. Prevalence of COVID-19-related risk factors and risk of severe influenza outcomes in cancer survivors: a matched cohort study using linked English electronic health records data. *EClinicalMedicine*. 2020; 29-30: 100656.

[28] Van den Driessche P, Watmough J. Reproduction numbers and sub-threshold endemic equilibria for compartmental models of disease transmission. *Mathematical Biosciences*. 2002; 180(1-2): 29-48.

[29] Ul Rehman A, Singh R, Agarwal P. Modeling, analysis and prediction of new variants of COVID-19 and dengue co-infection on complex network. *Chaos, Solitons & Fractals*. 2021; 150: 111008.

[30] WHO. *Background Paper on COVID-19 Disease and Vaccines: Prepared by the Strategic Advisory Group of Experts (SAGE) on Immunization Working Group On COVID-19 Vaccines*. World Health Organization; 2020.

[31] Visca D, Ong CW, Tiberi S, Centis R, D'ambrosio L, Chen B, et al. Tuberculosis and COVID-19 interaction: a review of biological, clinical and public health effects. *Pulmonology*. 2021; 27(2): 151-165.

[32] Chen Y, Wang Y, Fleming J, Yu Y, Gu Y, Liu C, et al. Active or latent tuberculosis increases susceptibility to COVID-19 and disease severity. *MedRxiv*. 2020. Available from: https://doi.org/10.1101/2020.03.10.20033795.

[33] Khurana AK, Aggarwal D. The (in) significance of TB and COVID-19 co-infection. *European Respiratory Journal*. 2020; 56(2): 32554537.

[34] Tadolini M, García García JM, Blanc FX, Borisov S, Goletti D, Motta I, et al. On tuberculosis and COVID-19 co-infection. *European Respiratory Journal*. 2020; 56(2): 2002328.

[35] Goudiaby MS, Gning LD, Diagne ML, Dia BM, Rwezaura H, Tchuenche JM. Optimal control analysis of a COVID-19 and tuberculosis co-dynamics model. *Informatics in Medicine Unlocked*. 2022; 28: 100849.

[36] Van den Driessche P, Watmough J. Further notes on the basic reproduction number. *Mathematical Epidemiology*. 2008; 8: 159-178.

[37] Routh EJ. *A Treatise on the Stability of a Given State of Motion, Particularly Steady Motion: Being the Essay to Which the Adams Prize Was Adjudged in 1877, in the University of Cambridge*. London: Macmillan and Company; 1877.

[38] Inayaturohmat F, Anggriani N, Supriatna AK. A mathematical model of tuberculosis and COVID-19 coinfection with the effect of isolation and treatment. *Frontiers in Applied Mathematics and Statistics*. 2022; 8: 958081.